DOI 10.1007/s11003-015-9851-7

Materials Science, Vol. 51, No. 3, November, 2015 (Ukrainian Original Vol. 51, No. 3, May–June, 2015)

INFLUENCE OF RRA TREATMENT ON THE MICROSTRUCTURE AND STRESS CORROSION CRACKING BEHAVIOR OF THE SPRAY-FORMED 7075 ALLOY

R.-M. Su,[1] Y.-D. Qu,[1,2] R.-D. Li,[1] and J.-H. You[1]

The effects of retrogression under pre-aging on the microstructure, mechanical properties, and stress corrosion cracking behavior of spray-formed 7075 aluminum alloys were investigated by the transmission electron microscopy, tensile tests, and slow strain rate tests. The results show that as a result of aging at 120°C for 16 h (as pre-aging), the strength of the alloy can be preserved on a high level and the grain-boundary precipitates are discrete after retrogression and re-aging treatment. However, the retrogression treatment is uncontrollable by the shortened retrogression period. After retrogression at 200°C for 8 min and re-aging, the ultimate tensile strength, elongation, and the stress corrosion cracking index of the alloy are 791 MPa, 8.5% and 0.155, respectively.

Keywords: spray forming, 7075 alloy, aging, retrogression, stress-corrosion cracking, strength.

The 7075 (Al–Zn–Mg–Cu) alloys are extensively used in the aerospace industry due to their desirable specific mechanical properties [1–4]. Since the application of the procedure of spray forming to 7075 alloy in the 1990s, its strength elevated to more than 730 MPa [5, 6]. Numerous papers reported the effects of heat treatments on 7075 alloy, which belong to the aging strengthening of aluminum alloy. Silva, et al. [7] and Ricker, et al. [8] report that both high strength and corrosion sensibility are obtained in 7075 aluminum alloys after the T6 treatment. The authors of [9–11] found the loss of strength of about 10–15% after the T73, T74, or T76 treatment in their studies of over-aging and the corrosion resistance of 7075 alloys.

For the contradiction between strength and corrosion resistance, Cina [12] (Israel Aircraft Industries, Ltd., 1974) presented a three-stage treatment (retrogression and re-aging, RRA). In the subsequent researches [13, 14], it was shown that the strength is maintained at the T6 level by the RRA treatment and that the stress corrosion cracking (SCC) resistance is close to T7 at the same time. Su, et al. [15, 16] reported that the RRA treatment can also improve the intergranular corrosion and exfoliation corrosion sensibility of the spray-formed 7075 alloy.

The RRA treatment consists of pre-aging, retrogression, and re-aging. Ohnishi [17, 18] considered the peak aging as the best pre-aging in the RRA treatment process. This type of pre-aging has been used until now. In recent years, the researchers report some different opinions. Thus, Lin [19] mentioned that the peak aging is not perfect pre-aging in a U.S. Patent and then Han, et al. [20] also made a similar conclusion. With regard for pre-aging in the RRA treatment, the arguments in the academia and studies concerning the type and reasons of pre-aging have not been reported yet.

The common retrogression is always treated at high temperatures and for short times (only dozens of seconds or even several seconds). Wu, et al. [21] and Reda, et al. [13] found that the sufficient retrogressed effects can be received by long-time retrogressions at a temperature below 200°C but the mechanical properties are lost at the same time.

[1] School of Material Science and Engineering, Shenyang University of Technology, Shenyang, China.

[2] Corresponding author; e-mail: quingdong@163.com.

Published in Fizyko-Khimichna Mekhanika Materialiv, Vol. 51, No. 3, pp. 68–75, May–June, 2015. Original article submitted February 17, 2014.

Hence, to offer the data on the optimization of aging treatment on spray-formed 7075 alloy and references for the next step of research, the present paper studies the effect of retrogression on the microstructure, mechanical properties, and SCC behavior of the spray-formed 7075 alloy under aging by the transmission electron microscopy (TEM), tensile tests, and slow strain-rate tests (SSRT).

Experimental

The experimental material was 7075 alloy with the following composition (wt. %): 5.48 Zn; 2.21 Mg; 1.48 Cu; 0.189 Cr; 0.371 Fe, and 0.121 Si.

The technological parameters of spray forming were as follows: the role of atomization gas was played by nitrogen (N_2); spraying distance of 370–380 mm, substrate eccentricity of 60–65 mm , conduit bore of 3.6 mm, angle of incidence of 37°–39°, spraying temperature of 770–780°C, crucible temperature of 735–745°C, horizontal velocity of 0.15 mm/sec, and vertical velocity of 0.18 mm/sec.

The bars after hot extrusion (temperature 400°C; ratio 30 : 1; rate 1.5 mm/sec) were processed into test samples 12.8 mm in diameter for two-stage solid solution (450°C for 1 h and 475°C for 2 h; water quenched to room temperature). The specimens were pre-aged at 120°C for 16 h, retrogressed at 160, 200, and 240°C for ~ 4 h, and re-aged at 120°C for 24 h.

The SCC behaviors were tested by the SCC-1 stress-corrosion experimental system corresponding to the ISO 7539-7: 2005 international standard (Corrosion of metals and alloys—Stress corrosion testing, Part 7: Method for slow strain rate testing); the strain rate was 10^{-6} sec^{-1} in dry air or in a 3.5 wt.% NaCl solution at 35 ± 1°C until cracking.

The disks for TEM observation 3 mm in diameter were punched out directly from the samples that were mechanically ground down to a thickness of 60 μm after aging. These disks were electropolished by using a DJ-2000 twin-jet electropolisher with a 30% nitric acid solution in methanol at – 30°C. The TEM examinations were performed with the help of a JEM-2100 transmission electron microscope.

Results

In Fig. 1, we show the ultimate tensile strength (UTS) and conductivity of the alloy during the retrogression at 160; 200 and 240°C and in the course of the corresponding re-aging. From Fig. 1, it can be seen that all tensile strength curves of retrogression first abruptly decline, then rise after falling to a certain degree, and finally again decline. Three tensile strength curves during retrogression have similar characteristics but the times of reaching the minimum and peak of strength are different, which depend on the retrogression temperatures. Since the diffusion rates of the solute and vacancies exhibit positive correlation with the retrogression temperature, this means that the time is shortened by higher retrogression temperatures.

The curves of tensile strength during the RRA are also similar. As the time of retrogression increases, the tensile strength first increases but then decreases after a peak value. The time of peak strength is between the minimum and the peak of tensile strength in the retrogression curve. As the retrogression temperature increases, the time of reaching the peak strength obviously shortens after the RRA. The strengths are also affected by the retrogression temperature. When the samples are retrogressed at 160°C, the peak tensile strength of the alloy after RRA is 772 MPa (Table 1). As the retrogression temperature increases, the tensile strength of the alloy gradually increases. If the samples are retrogressed at 200°C, the peak tensile strength of the alloy after RRA is 791 MPa. Then, as the retrogression temperature increases to 240°C, the peak tensile strength of the alloy after RRA is only 773 MPa, which is less than that after retrogression at 200°C.

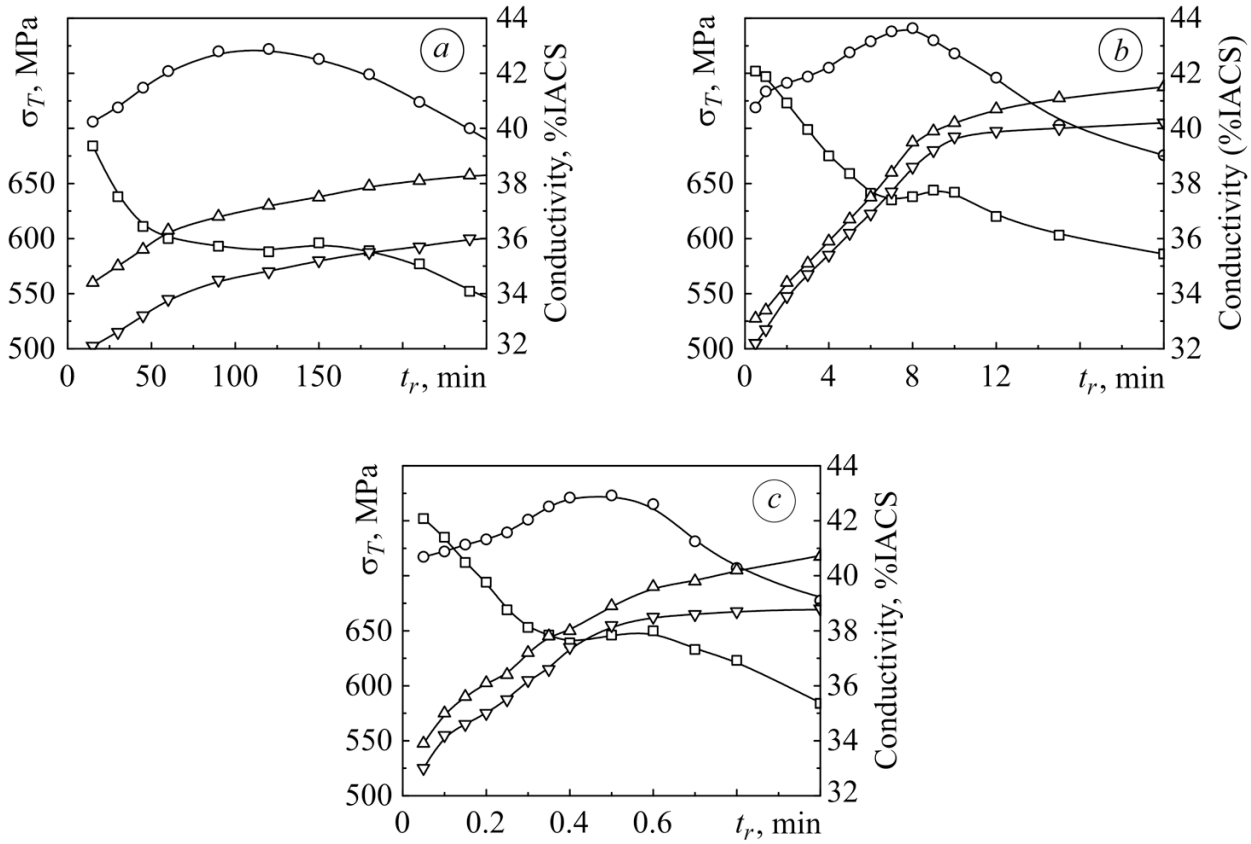

Fig. 1. Tensile strength and conductivity of the alloy in the course of retrogressions at 160°C (a), 200°C (b) and 240°C (c) and re-aging: (○, □) re-aged and retrogressed strength, respectively; (△, ▽) re-aged and retrogressed conductivity, respectively.

Table 1. Properties of the Alloy after Different Modes of Retrogression and Re-Aging Treatment

Pre-aging, °C × h	Retrogression, °C × min	Re-aging, °C × h	Conductivity, % IACS	UTS, MPa		Elongation, %		I_{SSRT}
				air	NaCl	air	NaCl	
120 × 16	160 × 120	120 × 24	37.2	772	710	8.8	6.6	0.287
120 × 16	200 × 8	120 × 24	39.5	791	756	8.5	7.4	0.155
120 × 16	240 × 0.5	120 × 24	38.8	773	737	8.6	7.7	0.136

It can also be seen that the conductivities first increase sharply and then gently with the time of retrogression. The behavior of conductivities is also influenced by the retrogression temperature. When the samples are retrogressed at 160°C, the variations of conductivity are small. In case of the retrogression above 200°C, the amplification of the conductivity is obvious. The conductivities can be improved up to 40% IACS and more.

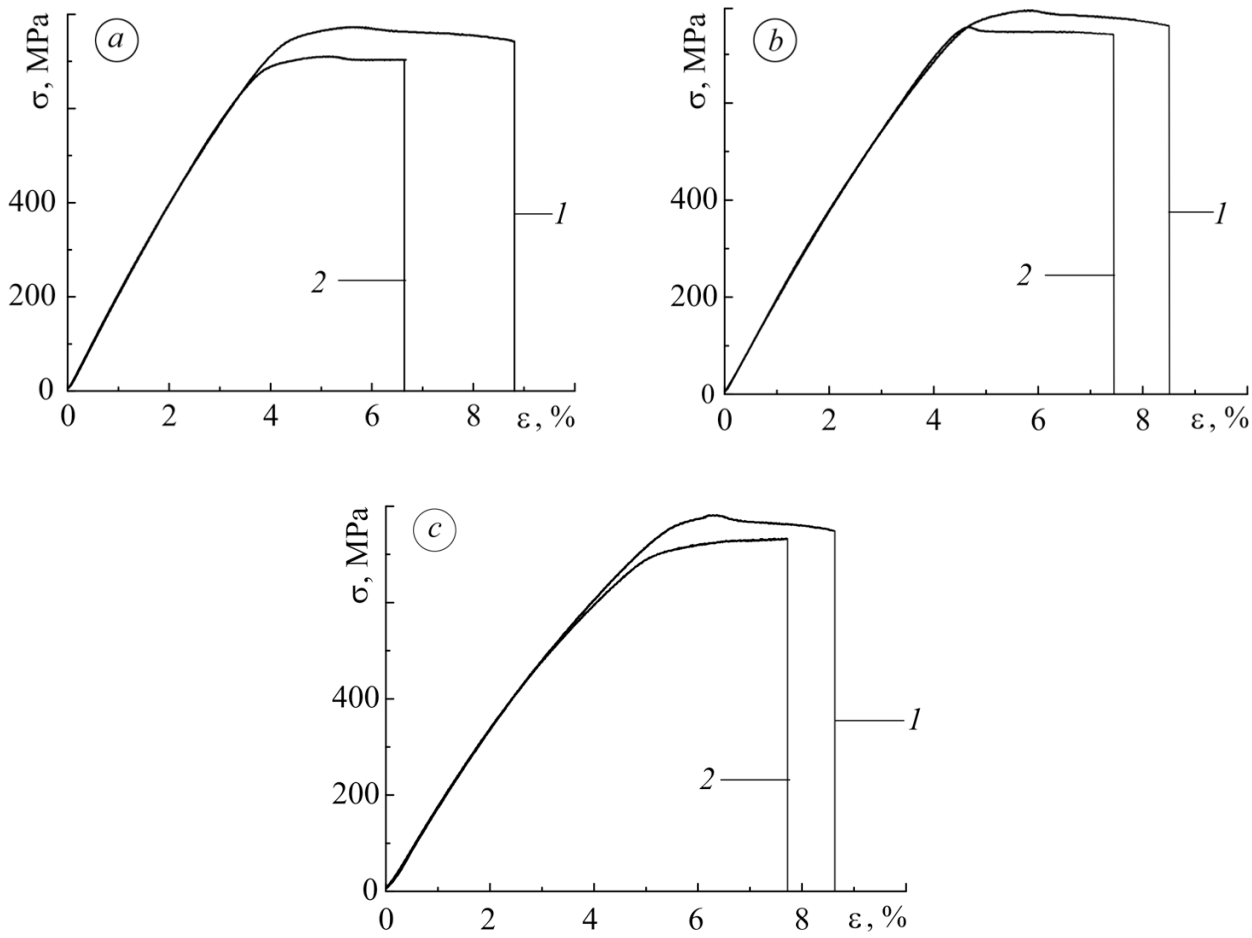

Fig. 2. SSRT stress-strain curves for the spray-formed 7075 alloy and different RRA treatments: (a) retrogression at 160°C for 120 min; (b) retrogression at 200°C for 8 min; (c) retrogression at 240°C for 0.5 min; (1) dry air; (2) 3.5 wt.% NaCl solution.

In Fig. 2, we show the SSRT stress-strain curves in dry air and in a 3.5 wt.% NaCl solution after three kinds of RRA treatment. It follows from Fig. 2 that the decrements of UTS in NaCl solutions are similar. However, the decrements of elongations observed in NaCl solutions after three kinds of RRA treatment are very different. As a result of the retrogression at 160°C for 120 min, the elongation falls down from 8.8% (in dry air) to 6.6% (in a 3.5 wt. % NaCl solution). This decrement of elongation constitutes 25%, which is much more than for the other RRA treatments with retrogression at 200°C and 240°C.

To judge the SCC resistance, the SCC index I_{SSRT} was introduced by processing various mechanical properties of SSRT:

$$I_{SSRT} = 1 - \frac{\sigma_{NaCl} \times (1 + \delta_{NaCl})}{\sigma_{air} \times (1 + \delta_{air})},$$

where σ_{NaCl} and σ_{air} are the UTS in a 3.5 wt.% NaCl solution and in dry air (MPa), respectively; δ_{NaCl} and δ_{air} are elongations in a 3.5 wt.% NaCl solution and in dry air (%), respectively. If the I_{SSRT} is close to 0, then the SCC resistance increases. The SSRT properties of spray-formed 7075 alloy after various modes of RRA treatments are also listed in Table 1.

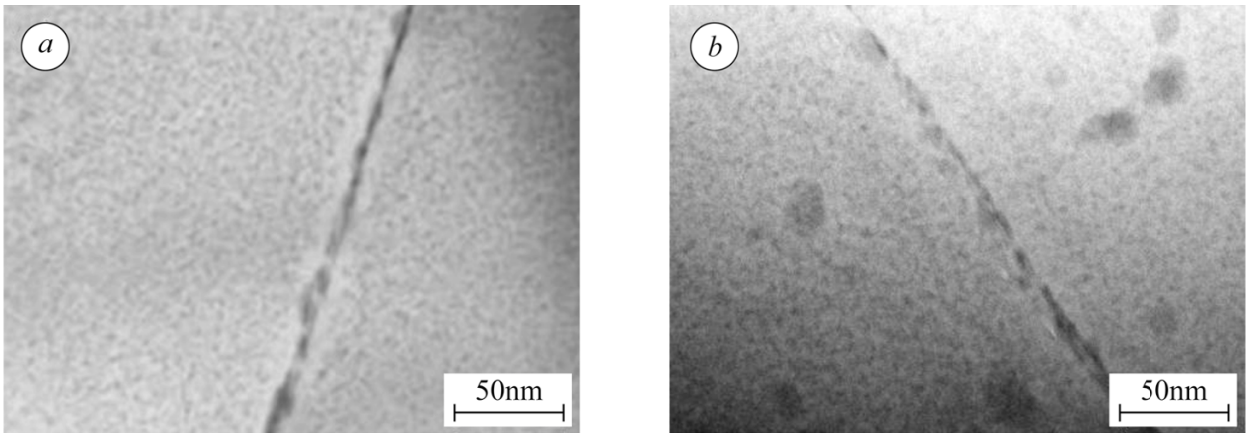

Fig. 3. TEM images of the alloy pre-aged at 120°C for 16 h (a) and 24 h (b).

Discussion

The ordinary precipitation sequence of 7xxx-series aluminum alloys can be summarized as follows [2]:

$$\text{SSS (super-saturated solid solution)} \rightarrow \text{GP zones} \rightarrow \text{metastable } \eta' \rightarrow \text{stable } \eta.$$

The GP zones are formed by metastable coherent solute clusters of Zn, Mg, and Cu. In the metastable η' phases, the Al, Cu and Mg components based on a solid solution of $MgZn_2$, $Mg(ZnCuAl)_2$, or $Mg(Zn_2, AlMg)$ appear as discrete platelet particles semicoherent with the matrix and known to populate inside the grains, and η is the same pseudostable noncoherent phase appearing as rods or plates, which are known to populate the grain boundary.

There is an intimate relationship between the microstructure and the properties of 7xxx series aluminum alloys. The properties of the 7xxx series aluminum alloys depend on the matrix precipitates (MP), grain-boundary precipitates (GBP), and precipitate-free zones (PFZ). According to the selected optimized process of heat treatment, the combined properties can be obtained by the cooperation of the above-mentioned three microstructures.

In microstructures, the strength of the alloy mainly relies on MP. In the entire aging process, the strength of the alloy changes with the characteristics of the GP zone, η', and η. The best strength depends on thin homogeneous dispersive MP. The plasticity, toughness, and SCC resistance of the alloy are remarkably influenced by the structure and chemical properties of GBP. There is a popular belief that continuous GBP are harmful for the properties of alloys. Since the relative motion of crystalline grains in the process of deformation is impeded by continuous GBP, the plasticity and toughness of the alloy are completely injured. On the other hand, the continuous GBP are preferentially dissolved as anodes in the anodic dissolution theory. Since the potentials of GBP, PFZ, and matrix are equal to -1.05 V, -0.85 V, and -0.75 V, respectively, the potential difference (PD) between the GBP and the PFZ is smaller than the PD between the GBP and the matrix [22]. As for the SCC resistance of the alloy, the effect of widening of the PFZ can remit the SCC sensibility and improve the SCC resistance of the alloy.

In Fig. 3, we show the TEM images of the alloy pre-aged at 120°C for 16 h and 24 h. From Fig. 3a, it can be found that the MPs are small and rare after early aging at 120°C for 16 h. Since precipitation is deficient, the GBPs are small, continuous, and semicontinuous.

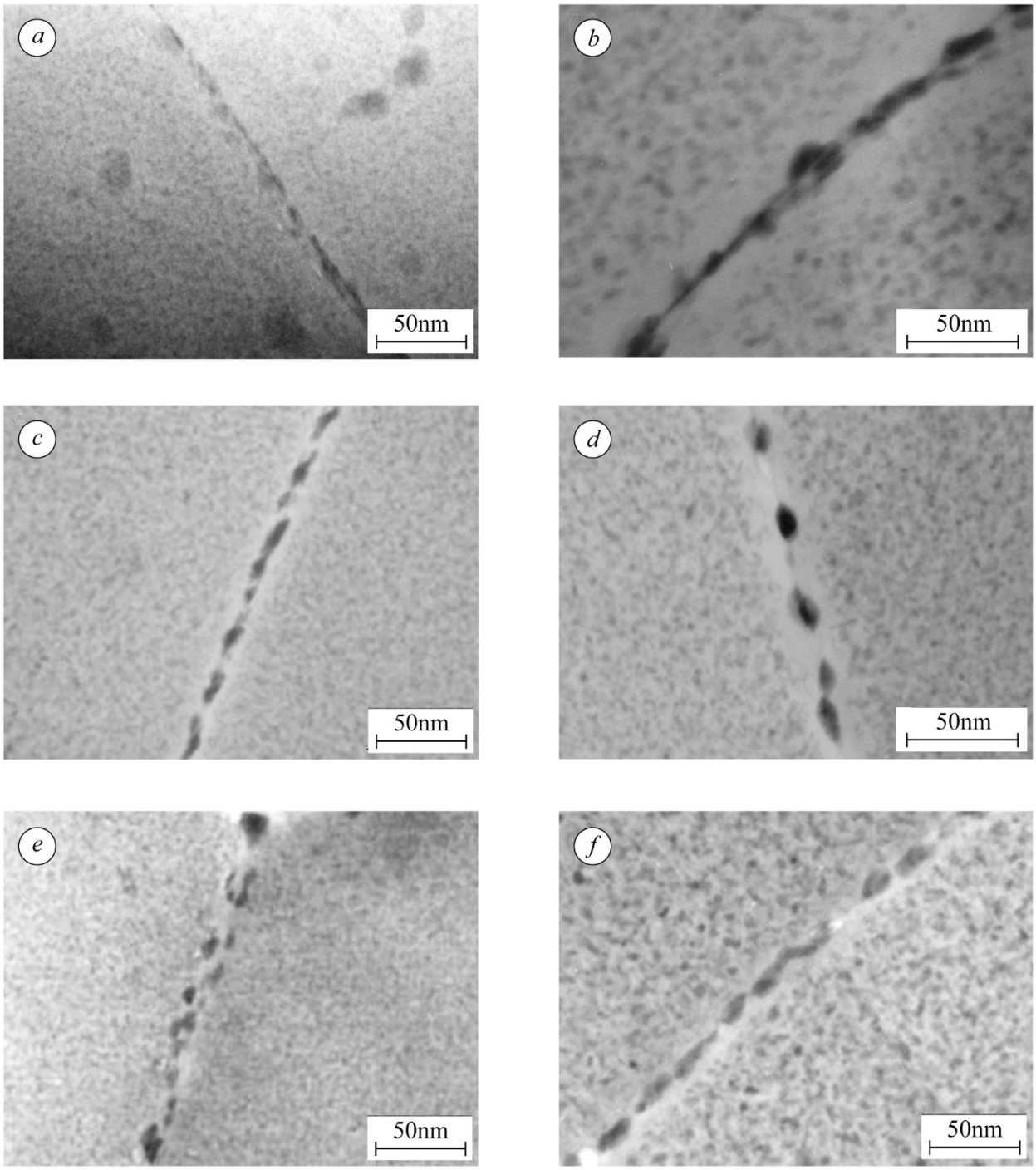

Fig. 4. TEM images of the alloy after different retrogression and re-aging treatments via pre-aging: (a, b) retrogressed at 160°C for 120 min and re-aged, respectively; (c, d) retrogressed at 200°C for 8 min and re-aged, respectively; (e, f) retrogressed at 240°C for 0.5 min and re-aged, respectively.

After the T6 treatment (120°C for 24 h), the MPs are dispersively distributed, mostly 1–2 nm in size, but with some big precipitates more than 10 nm in size (they are formed by precipitates growing in the course of aging) (Fig. 3b); the GBPs are discrete but close, like a chain. There are few PFZ on the grain boundaries after

pre-aging treatments. The continuous or chain-shaped GBPs are harmful to the SCC resistance of the alloy and, hence, the SCC sensibility is high in the 7075 alloy for the T6 treatment.

In Fig. 4, we show the TEM images of the alloy after different retrogression and re-aging treatments. The MP are only partly redissolved in the matrix after retrogression at a low temperature (160°C) via pre-aging at 120°C for 16 h; the GBPs are discrete, and the obvious PFZ are left on the grain boundaries (Fig. 4a). After RRA with pre-aging and low temperature retrogression, thin homogeneous dispersed MPs are again separated in the matrix. Their average sizes are smaller than 5 nm. The PFZ width is 15–20 nm.

After the RRA treatment (Fig. 4b), in view of the high strength of the material, the MP are separated by elements of the alloy, where large numbers of MPs (smaller than the critical dimension) are dissolved in the course of the retrogression treatment. The GBPs are thick and discrete. Those GBPs may serve as an obstacle to the formation of galvanic corrosion and improve the corrosion resistance of the alloy. The available data shows that the conductivity increases but the SCC index I_{SSRT} decreases [23].

It is easy to see (Fig. 4c) that most of the MPs are redissolved in the matrix after retrogression at 200°C. A part of GBP is redissolved, whereas the remaining GBPs grow along the grain boundaries. Thus, the GBPs are long and discrete. After re-aging, the MPs are thin, homogeneous, and dispersed, while the GBPs are obviously rounded and discrete. The MP size is about 2 nm. The average size and spacing of the GBP is 5–7 nm and more than 10 nm, respectively (Fig. 4d). The SCC resistance of the alloy is improved by the indicated discrete GBPs.

In the case of retrogression at 240°C (Fig. 4e), the situation with MP mostly redissolved in the matrix is similar to the situation observed after retrogression at 200°C. However, the morphology of the grain boundary is different. The GBPs are semicontinuous, the sizes and spacing of the GBPs are small, and some GBP are arranged side by side. After re-aging, the MPs are coarsened and grown. Their sizes increase from 1–2 nm to 3–5 nm. The GBPs are still semicontinuous but the phenomenon of GBP arranged side by side disappeared. The PFZ are widened to 5 nm but they are still less narrow than for the other effects of retrogression treatments, as shown in Fig. 4f. The SCC resistance of the alloy can be improved to a certain extent by above-mentioned grain-boundary structures.

The short time of retrogression at 240°C is the main factor affecting the properties of the alloy after RRA treatment. Since the retrogression time constitutes only dozens of seconds, we may observe the phenomena of nonuniform heat treatment of the samples, e.g., for thin sheets. When the optimal effect is discovered on the surface of the sample, the interior of the sample is still incompletely treated. When the bulk of the sample is suited by retrogression, the surface of the sample may become overtreated. Hence, the strength, conductivity, and SCC index I_{SSRT} of the alloy via retrogression at 240°C are not better than for the other retrogression treatments.

CONCLUSIONS

In the case of aging at 120°C for 16 h (realized as pre-aging in the RRA treatment), the following conclusions can be made concerning the analyzed three modes of retrogression treatment of the spray-formed 7075 alloy:

— most of the matrix precipitates (MP) are redissolved in the matrix and the grain boundary precipitates (GBP) are obviously discrete after the retrogression at 200°C for 8 min; after re-aging, the UTS, elongation, and SCC index of the alloy are 791 MPa, 8.5% and 0.155, respectively.

— The MPs are only partly redissolved in the matrix after retrogression at the low temperature (160°C); the GBPs are discrete and the obvious PFZ are located on the grain boundaries; after the RRA with

low-temperature retrogression, thin homogeneous dispersed MP are also separated in the matrix and their average sizes are smaller than 5 nm.

— The MPs separated in the matrix during pre-aging are efficiently redissolved and the GBP is interrupted by retrogression at 240°C; however, the procedure of retrogression lasting for dozens of seconds is hardly controlled; there are some differences in the degree of treatment between the surface and the bulk of the sample and, hence, the properties of the alloy after RRA are not perfect.

– the SCC index I_{SSRT} is affected by the combined action of GBP and PFZ; continuous GBPs and narrow PFZ increase the SCC susceptibility of the alloy and its SCC index I_{SSRT}; however, the discrete GBP and wide PFZ can improve the SCC resistance of the alloy and decrease its SCC index I_{SSRT}.

Acknowledgements. The present research was financially supported by the Program for Liaoning Innovative Research Team in University (LT2012004) and the Fok Ying-Tong Education Foundation (121054).

REFERENCES

1. T. Hu, K. Ma, T. D. Topping, J. M. Schoenung, and E. J. Lavernia, "Precipitation phenomena in an ultrafine-grained Al alloy," *Acta Mater.,* **61**, 2163–2178 (2013).
2. S. L. George and R. D. Knutsen, "Composition segregation in semi-solid metal cast AA7075 aluminum alloy," *J. Mater. Sci.,* **47**, 4716–4725 (2012).
3. T. Marlaud, A. Deschamps, F. Bley, et al., "Influence of alloy composition and heat treatment on precipitate composition in Al–Zn–Mg–Cu alloys," *Acta Mater.,* **58**, 248–260 (2010).
4. T. Marlaud, A. Deschamps, F. Bley, et al., "Evolution of precipitate microstructures during the retrogression and re-aging heat treatment of an Al–Zn–Mg–Cu alloy," *Acta Mater.,* **58**, 4814–4826 (2010).
5. R. M. Su, Y. D. Qu, R. X. Li, and R. D. Li, "Study of aging treatment on spray forming Al–Zn–Mg–Cu alloy," *Appl. Mech. Mater.,* **217**, 1835–1838 (2012).
6. M. Jeyakumar, S. Kumar, and G. S. Gupta, "Microstructure and properties of the spray-formed and extruded 7075 Al alloy," *Mater. Manuf. Proc.,* **25**, 777–785 (2010).
7. G. Silva, B. Rivolta, R. Gerosa, and U. Derudi, "Study of the SCC behavior of 7075 aluminum alloy after one-step aging at 163°C," *J. Mater. Eng. Perform.,* **22**, 210–214 (2013).
8. R. E. Ricker, E. U. Lee, R. Taylor, et al., "Chloride ion activity and susceptibility of Al alloys 7075-T6 and 5083-H131 to stress corrosion cracking," *Metall. Mater. Trans. A,* **44**, 1353–1364 (2013).
9. G. Zhang, Z. Chen, X. Zhu, et al., "The heat treatment behavior of super-high strength aluminum alloys by spray forming," *J. Mater. Sci. Chem. Eng.,* **1**, 57–60 (2013).
10. H. Fooladfar, B. Hasnemi, and M. Younesi, "The effect of the surface treating and high-temperature aging on the strength and SCC susceptibility of 7075 aluminum alloy," *J. Mater. Eng. Perform.,* **19**, 852–859 (2010).
11. E. M. Arnold, J. J. Schubbe, P. J. Moran, and R. A. Bayles, "Comparison of SCC thresholds and environmentally assisted cracking in 7050-T7451 aluminum plate," *J. Mater. Eng. Perform.,* **21**, 2480–2486 (2012).
12. B. M. Cina, *U. S. Patent 3856584. Reducing the Susceptibility of Alloys, Particularly Aluminum Alloys, to Stress Corrosion Cracking,* (1974).
13. Y. Reda, R. Abdel-Karim, and I. Elmahallawi, "Improvements in mechanical and stress corrosion cracking properties in Al-alloy 7075 via retrogression and re-aging," *Mater. Sci. Eng. A,* **485**, 468–475 (2008).
14. G. Peng, K. Chen, S. Chen, and H. Fang, "Influence of repetitious-RRA treatment on the strength and SCC resistance of Al–Zn–Mg–Cu alloy," *Mater. Sci. Eng. A,* **528**, 4014–4018 (2011).
15. R. M. Su, Y. D. Qu, and R. D. Li, "Effect of aging treatments on the mechanical and corrosive behaviors of spray-formed 7075 alloy," *J. Mater. Eng. Perform.,* **23**, 3842–3848 (2014).
16. R. M. Su, Y. D. Qu, R. D. Li, et al., "Effect of aging treatments on microstructure and exfoliation corrosion behavior of spray forming 7075 alloy," *Adv. Mater. Res.,* **774**, 872–875 (2013).
17. T. Ohnishi, Y. Ibaraki, and T. Ito, "Improvement of fracture toughness in 7475 aluminum alloy by the RRA (retrogression and re-aging) process," *Mater. Trans. JIM,* **30**, 601–607 (1989).

18. K. Higashi, T. Ohnishi, and I. Tsukuda, *U. S. Patent 4713216 K. Aluminum Alloys Having High Strength and Resistance to Stress and Corrosion* (1987).
19. J. Lin, and M. M. Kersker, *U. S. Patent 5108520J. Heat Treatment of Precipitation Hardening Alloy* (1992).
20. X. L. Han, B. Q. Xiong, Y. A. Zhang, et al., "Triple over-aging treatment of 7150 aluminum alloy," *Chin. J. Nonferrous Met.,* **22**, 3006–3014 (2012).
21. X. J. Wu, M. D. Raizenne, R. T. Holt, et al., "Thirty years of retrogression and re-aging (RRA)," *Can. Aeron. Space J.,* **47**, No. 3, 131–138 (2001).
22. F. X. Song, X. M. Zhang, S. D. Liu, et al., "Effect of aging on corrosion resistance of 7050 aluminum alloy pre-stretching plate," *Chin. J. Nonferrous Met.,* **23**, 645–651 (2013).
23. D. Wang, D. R. Ni, and Z. Y. Ma, "Effect of pre-strain and two-step aging on microstructure and stress corrosion cracking of 7050 alloy," *Mater. Sci. Eng. A,* **494**, 360–366 (2008).